Respiratory Entrainment of Units in the Mouse Parietal Cortex Depends on Vigilance State

Felix Jung
Heidelberg University
Yevgenij Yanovsky
Heidelberg University
Jurij Brankačk
Heidelberg University
Adriano BL Tort
Federal University of Rio Grande do Norte
Andreas Draguhn (andreas.draguhn@physiologie.uniheidelberg.de)
Heidelberg University

Research Article

Keywords: posterior parietal cortex, unit firing, respiration, θ rhythm, sleep, wakefulness

Posted Date: March 17th, 2022

DOI: https://doi.org/10.21203/rs.3.rs-1445724/v1

Abstract

Synchronous oscillations are essential for coordinated activity in neuronal networks and, hence, for behavior and cognition. While most network oscillations are generated within the central nervous system, recent evidence shows that rhythmic body processes strongly influence activity patterns throughout the brain. A major factor is respiration, which entrains multiple brain regions at the mesoscopic (local field potential) and single-cell levels. However, it is largely unknown how such respiration-driven rhythms interact or compete with internal brain oscillations, especially those with similar frequency domains. In mice, respiration and theta (θ) oscillations have overlapping frequencies and co-occur in various brain regions. Here we investigated the effects of respiration and θ on neuronal discharges in the mouse parietal cortex during four behavioral states which either show prominent θ (REM sleep and active waking (AW)) or lack significant θ (NREM sleep and waking immobility (WI)). We report a pronounced state-dependence of spike modulation by both rhythms. During REM sleep, θ effects on unit discharges dominate, while during AW respiration has a larger influence, despite the concomitant presence of θ oscillations. In most states, unit modulation by θ or respiration increases with mean firing rate. The preferred timing of respiration-entrained discharges (inspiration versus expiration) varies between states, indicating state-specific and different underlying mechanisms. Our findings show that neurons in an associative cortex area are differentially and state-dependently modulated by two fundamentally different processes: brain-endogenous θ oscillations and rhythmic somatic feedback signals from respiration.

Introduction

Neuronal network oscillations are important for coordinating multi-neuronal activity patterns within and across different brain regions [15]. Multiple lines of evidence show that such coordinated patterns, in turn, are a key mechanism underlying cognition and behavior [17, 18, 24]. While most oscillation patterns result from brain-endogenous network dynamics, there is growing evidence that they can also be generated or modulated by feedback from rhythmic activity in the body. Such rhythmic feedback signals include respiration [23, 29, 57], cardiac activity [13, 25, 60] and the gastric rhythm [45, 46]. Modulation of neuronal behavior occurs across species, including humans [26, 64], and it affects widespread regions of the brain [47, 57]. Respiration-driven oscillations are not only visible at the network level but do modulate spiking of single neurons in different regions including frontal cortex [5, 35], dentate gyrus [12] and parietal cortex [32]. In line with these findings, several lines of evidence show that oscillating somatic feedback signals affect cognition in humans [41, 64] and rodents [4, 23].

Neuronal network oscillations cover a large range of frequency bands, and different oscillation patterns occur in different functional states of the brain which, in turn, reflect specific cognitive-behavioral states of the organism [15]. This raises the question of how brain-endogenous and somatically generated oscillations co-occur and interact. A recent example illustrates the complexity of such interactions: brain-endogenous theta (θ, 5–12 Hz) strongly modulate local gamma (γ, 40–160 Hz) oscillations, a fundamental pattern for cortical computation and cognition [6, 10, 17, 37, 41, 55, 56]. Recordings from

freely behaving mice have shown that the prominent θ-γ-coupling during REM sleep [48] is modulated by respiration rate, expressing maximum coupling at a moderate respiration frequency of around 5 Hz [20]. This modulation may be associated to an intermediate level of arousal which is reflected by breathing frequency during REM sleep [54, 62].

Thus, brain-endogenous and body rhythms show complex, state-dependent interactions which are likely to be functionally relevant. It is therefore important to untangle the effects of different oscillations on neuronal discharges, especially in regions where oscillations with overlapping frequency bands co-occur. This is the case for θ- and respiration-related (RR) oscillations in cortical networks of the mouse [12, 63]. Here, we studied the impact of both oscillation patterns on neuronal discharge behavior in the posterior parietal cortex, a multi-modal associative area with known modulation by both θ [51] and respiration [32]. As a reference signal for respiratory activity ('Resp'), we measured rhythmic pressure fluctuations in a plethysmograph, which is much more stable than the fluctuating field potentials reflecting RR[30]. Unit activity was recorded in two vigilance states with prominent θ activity (active waking and REM sleep) and in two states without significant θ power (waking immobility and non-REM sleep (NREM)). Our results reveal a strong modulation of unit discharges by both θ and Resp. The relative impact of either oscillation differs among states, suggesting different and independent functions of brain-endogenous and somatic feedback-generated oscillations for cognition and behavior.

Material And Methods

All procedures complied with guidelines of the European Science Foundation and the US National Institute of Health Guide for the Care and Use of Laboratory Animals, and were approved by the State Supervisory Panel on Animal Experiments of Baden-Württemberg (35–9185.81/G-84/13, 35-9185.81/G-137/17, 35-9185.81/G-44/16). Parts of the data recorded during REM sleep and waking immobility have been previously published in a different context [32].

Animal care and housing

Mice of the C57BL/6N strain were obtained from Charles River and housed inside a ventilated Scantainer with an inverted 12/12 hour light-dark cycle (light on at 8:00 p.m.) and free access to water and food.

Surgery and electrode implantation

A total of thirteen male mice weighing 23–30 g (13–21 weeks old) were anesthetized with a mixture of isoflurane and medical oxygen (4% isoflurane for induction, 1.5–2.5% for maintenance). In 10 animals, between 5 to 7 tetrodes were chronically implanted into the right and left parietal cortex at various depths (2 mm posterior bregma, 1.5 mm lateral, 0 to 0.8 mm ventral). In three animals, 16-channel silicon probes (A1x16-3mm-50-177-CM16LP; NeuroNexus Technologies) were chronically implanted into the right parietal cortex. Inter-electrode distance was 50 µm, and implantation was perpendicular to the cortical surface such that the uppermost electrode was located superficially, the lowest at 750 µm). For further details, see [32].

Electrophysiology in freely moving mice

After one week of recovery, the animals were habituated to a whole-body plethysmograph (EMKA Technologies, S.A.S., France; [20, 30] which was adapted for simultaneous recording of respiration (Resp) and brain electrophysiology. Although respiration-related rhythms (RR) are detectable in the parietal cortex [57], they vary strongly depending on vigilance states, respiration frequency [19, 30], and other hitherto unknown factors. To avoid signal instabilities due to this variability of RR, we used the Resp signal instead, which is directly derived from respiration-induced pressure changes in the plethysmograph (see Methods) and remains stable throughout all vigilance states. Movements were detected with 3-D accelerometry. Animals were recorded in several sessions of up to 4 hours on consecutive days.

Behavioral staging

Artifact-free periods of recorded potentials were visually identified. Animals with linear silicon probes had excessive amounts of movement artefacts during active waking. We therefore limited analysis of this particular state to the remaining 10 animals with implanted tetrodes. Behavioral and vigilance state was assessed according to accelerometer activity (active waking > wake immobility or sleep), slow-wave activity (NREM > wake immobility, active waking, REM) and regular θ rhythm (preset in REM and active waking). For further details, see [7].

Data analysis

Built-in and custom-written routines in MATLAB (The MathWorks) were used for data analysis. For analysis of power spectral density, we used the *pwelch.m* function (50% overlap, 4-s Hamming windows). Spike detection, sorting and quality assessment was done using the sorting algorithm "*Wave_clus*" [11, 44], similar to [32]. Units with fewer than 100 spikes during the total recording time were excluded. Four quality tests were applied to the initial results of sorting: 1) the Hill test [27]: <1% of detected spikes occur within the first 1 ms after a spike; 2) isolation distance [21], which estimates the distance of each cluster to other clusters (> 15); 3) cluster quality L_{ratio} (< 0.25). L specifies the degree of separation between two clusters, a low value of L indicates that the cluster is well separated. However, clusters may be of different size and L divided by the number of spikes (L_{ratio}) allows larger clusters to tolerate more contamination [49]; 4) correlation coefficient ($r < 0.98$) between spike waveforms for each unit across all recording sites (four for tetrodes and three for probes). *Firing rates*: Periods of non-spiking (larger than the longest inter-spike interval which was validated for each unit by using all spikes) and bursts (intra-burst interval of 5 ms and less) were excluded from the calculation of firing rates. *Spike-field coupling*: Phase time series were obtained by using the *hilbert.m* function (for details, see [32]). Spike-phase distributions were then calculated by relating the spike times with the instantaneous phases of the oscillating field potential. The *Rayleigh test* for uniformity of circular distributions was used to check for statistical significances. Coupling strength to Resp and θ was estimated using the circular mean resultant length (R).

Histology

After the last experiment, the animals were deeply anaesthetized with ketamine-xylazine (30mg/kg + xylazine 10 mg/kg) and perfused transcardially with PBS followed by 4% paraformaldehyde. The position of tetrodes and multichannel probes was then verified by fluorescence (staining with DAPI: 4,6-Diamidin-2-phenylindol) and light microscopy. For further details, see [32].

Statistics

Data are presented as means ± SEM for Gaussian distributions or as medians ± 25/75% percentiles for non-Gaussian distributions. The *Mann Whitney U test* was applied for comparing coupling strength. For comparisons of proportions, the *Chi-squared test* was used. Two-sample testing of circular data was performed with the Watson's U2 test. p values of < 0.05 were considered as statistically significant.

Results

We recorded field potentials and respiration (Resp) from 13 freely behaving male mice (see Methods). In line with previous publications [7, 57, 65], we found a strong state-dependence of θ oscillations and slow-wave activity in the posterior parietal cortex: During REM sleep and in active waking (AW), local field potentials (LFP) were dominated by θ. In contrast, high voltage slow waves were characteristic during NREM sleep. During waking immobility (WI), both slow waves and θ were absent.

Unit firing is modulated by respiration

The presence of respiratory rhythms (RR) in the parietal cortex depends on behavioral states [57] and varies strongly with respiration frequency [30] and probably further factors [19]. We therefore used the respiration (Resp) signal from plethysmography which could be reliably recorded during all four behavioral or vigilance states (see Methods). In the θ–containing states (AW, REM), however, the effects of Resp and θ on neuronal activity could only be separated when the oscillations exhibited different frequencies. Figure 1A shows an example recording during AW with Resp rates exceeding and partly overlapping the frequency of θ in the LFP (see power spectral densities in Fig. 1B). In this example, we illustrate the detection, waveform and rhythmic modulation of an identified unit (Fig. 1C-F). This unit is significantly coupled to respiration when the breathing frequency is > 4 Hz (fast respiration, coupling strength R = 0.123, Fig. 1D). In this situation, firing probability is highest between maxima of expiration (Ex, 90 deg) and inspiration (In, 270 deg, Fig. 1E). At the same time, this example unit is not modulated by θ (5–15 Hz, Fig. 1F; for modulation by slow respiration see below). Similar analyses were applied to all recorded units in all animals and states (n = 1543), giving a systematic account of state-dependent unit entrainment by θ and Resp.

Unit coupling depends on vigilance state

Power spectral densities of Resp and θ were largely overlapping in AW (Fig. 2A right panel) and partially overlapping in REM (Fig. 2A left panel), whereas θ was absent in NREM and WI (Fig. 2A middle panels). Depending on vigilance state, the animal's breathing frequency varied strongly between 1 and 14 Hz. For further analysis, we differentiated between slow (1–4 Hz) and fast (> 4 Hz) Resp. Both slow (sR) and fast

Resp (fR) were present in REM and WI. In contrast, NREM contained almost exclusively sR, and AW almost exclusively fR. The variability in breathing rate reflects the differences in vigilance and in physical activity among the respective states. The percentage of units modulated by θ, sR, fR or by both θ and Resp simultaneously (referred to as “both” units) varied among vigilance states (Fig. 2B). As expected, the percentage of units modulated by any of the slow rhythms (θ and Resp, pooled) was significantly higher in states with θ present compared to non-θ states (see Table 1 for details). Moreover, the percentage of units coupled to Resp and both Resp and θ simultaneously was larger in AW compared to REM. Interestingly, in spite of the presence of θ in both states, significantly more units were modulated by θ in REM compared to AW. In contrast, significantly more units were modulated by Resp in AW compared to REM. Finally, coupling percentage to Resp was not different between WI and NREM. In summary, the coupling of units to θ or Resp is highly state-dependent. More units are modulated by θ in REM whereas more units are modulated by Resp in AW.

Unit coupling depends on firing rate

Next we analyzed whether unit coupling to θ or Resp was influenced by the mean firing rate (FR). For estimation of FR, bursts and spiking gaps were excluded (see Methods). We found that the percentage of units coupled to θ or Resp varied with FR in a state-dependent manner. During REM, coupling percentage to θ increased with increasing FR (Fig. 2C left, see details in Table 1); in contrast, during AW the percentage of coupled units showed a non-significant trend to decrease (Fig. 2C right). Coupling to Resp increased with FR in REM, NREM and AW but not in WI (Fig. 2C and Table 1). In conclusion, unit coupling to either rhythm varies with FR, but this correlation depends on behavioral or vigilance state.

Coupling strength depends on vigilance state.

We next measured the strength of coupling between individual units and the underlying oscillations. Table 1 shows the outcome of statistical tests for the most relevant comparisons. We found that coupling strength for units exclusively coupled to θ (and not Resp) was higher in REM compared to AW (Fig. 2D left). Coupling strength to sR was lower in NREM compared to REM and WI (Fig. 2D). In WI, coupling strength to fR was higher than to sR (Fig. 2D). Coupling strength to fR was highest in WI compared to REM and lowest in AW (Fig. 2D right). In all, we conclude that coupling strength differs among vigilance states, between the two types of slow rhythms, and also with respiration frequency.

Unit firing and phase preference.

Finally, we looked for phase preference of units modulated by θ or Resp and found pronounced state-specific differences. Preference to θ phase differed between REM and AW (Fig. 3A). Preference to either inspiration or expiration in units coupled to sR was different in NREM compared to REM and WI (Fig. 3B, upper row). For units modulated by fR, Resp phase preference differed in all three states: REM, WI and AW (Fig. 3B, lower row). For statistics, see Table 1.

Table 1

Details of unit behavior. AW: active waking; WI: wake immobility; NREM: non-REM sleep; REM: REM sleep; Both: units modulated by and respiration simultaneously; : units modulated by ; Resp: units modulated by respiration; fR: units modulated by fast respiration; sR: units modulated by slow respiration; None: units not modulated, neither by nor by respiration.

Overview of statistical differences			
Percentage of units with coupling to θ or Resp			
Unit type	*Property*	*Test*	*p*
All except None	θ-states > non-θ states	Chi-square	< 0.0001
All except None	REM < AW	Chi-square	0.0017
θ + Both	REM > AW	Chi-square	0.0007
Resp + Both	REM < AW	Chi-square	< 0.0001
Resp + Both	WI = NREM	Chi-square	0.6541
Dependence of coupling on firing rate			
Unit type	*State*	*Property*	*Test*	*p*
θ + Both	REM	↑ with firing rate	Chi-square	< 0.0001
θ + Both	AW	no change	Chi-square	0.9971
Resp + Both	REM	↑ with firing rate	Chi-square	0.003
Resp only	NREM	↑ with firing rate	Chi-square	< 0.0001
Resp only	AW	↑ with firing rate	Chi-square	0.0008
Resp only	WI	no change	Chi-square	0.1052
Coupling strength			
Unit type	*Rhythm*	*Property*	*Test*	*p*
θ only	θ	REM > AW	Mann-Whitney	0.0136
Both	θ	REM = AW	Mann-Whitney	0.9476
sR only	Resp	REM > NREM	Dunn's multiple comparison	< 0.0001
sR only	Resp	REM = WI	Dunn's multiple comparison	0.9999
sR only	Resp	NREM < WI	Dunn's multiple comparison	< 0.0001
fR only	Resp	REM > AW	Dunn's multiple comparison	< 0.0001
fR only	Resp	WI > AW	Dunn's multiple comparison	< 0.0001
fR only	Resp	REM = WI	Dunn's multiple comparison	0.4658

Overview of statistical differences				
State	*Rhythm*	*Property*	*Test*	*p*
REM	θ	θ only > Both	Mann-Whitney	0.0028
WI	Resp	sR only < fR only	Mann-Whitney	0.0013
REM	Resp	sR only = fR only	Mann-Whitney	0.9421
Phase preference				
Unit type	*Property*		*Test*	*p*
θ + Both	REM vs. AW/ different		Watson U^2	< 0.0001
sR only	REM vs. NREM/ different		Watson U^2	< 0.0001
sR only	NREM vs. WI/ different		Watson U^2	< 0.0001
sR only	REM vs. WI/ not changed		Watson U^2	0.1955
fR only	REM vs. WI/ different		Watson U^2	0.0223
fR only	REM vs. AW/ different		Watson U^2	0.0058
fR only	WI vs. AW/ different		Watson U^2	< 0.0001

Discussion

Our data shows specific and robust modulation of units in the parietal cortex by both respiration and θ. However, the rhythmic entrainment of units by either of the two slow oscillations depends strongly on (i) vigilance state and (ii) mean firing rate (FR). In order to gain a systematic overview, we compared all major sleep and waking states. In two of these states, active waking (AW) and REM sleep, both oscillations are simultaneously present. At the field potential level θ oscillations are dominant in both states. At the cellular (unit) level, however, entrainment by respiration is prevailing during AW while θ is more efficient during REM sleep. This observation emphasizes potential discrepancies between the observed power of network-level oscillations and behavior of individual neurons which should be kept in mind when interpreting collective neuronal signals (field potentials, EEG, MEG). A second finding of the present study is that in several states coupling of units to θ or Resp, respectively, was dependent on discharge frequency. Whether this activity-dependence of entrainment reflects differences in network integration of different cell types or of differentially active neurons of the same type is presently unclear. In any case, the correlation between neuronal activity and coupling to slow network oscillations may be important for understanding ensemble activity in oscillating networks. A further new observation is that units couple to different phases of respiration depending on the behavioral state. This finding may be explained by state-dependent differences in respiration-related synaptic input to the parietal network, by

recruitment of different types of interneurons within the parietal cortex, or by other, more complex state-dependent interactions between different networks. In any case, all findings underline the strong state-dependence of unit entrainment by both, respiration and θ oscillations.

Some of the present findings from freely moving mice confirm our earlier results from head-fixed [12] and urethane-anaesthetized animals [63]. In these preparations, we had already reported respiration-driven modulation of hippocampal [57, 63] and posterior parietal and prelimbic neurons [32, 65]. While our previous observations were mainly done in REM sleep or wake immobility, we here provide a systematic comparison of modulation by θ and respiration during all major states of vigilance/behavior: REM sleep, NREM sleep, waking immobility and active waking. The latter is of particular interest since it contains θ oscillations and, at the same time, strong respiration-coupled inputs from sniffing behavior. In this state, entrainment of neurons by respiration was dominant, with particularly strong effects on neurons with high discharge frequency. It is well feasible that this reflects the integration of sensory signals from nasal respiration or sniffing in the multimodal association network of the parietal cortex.

Earlier reports have shown that neurons in several neocortical regions including the parietal cortex of rats and mice are modulated by theta oscillations during locomotion and REM sleep [51]. Here, we confirm this finding for REM sleep while foraging behavior could not be tested within the limited space inside the plethysmograph. During active waking, neurons were entrained by both θ and respiration (sniffing), with dominant modulation by respiration. A similar concomitant modulation of neurons by θ and respiration has been described by Biskamp and colleagues for medial prefrontal cortex neurons in mice [5]. It may well be that theta becomes more efficient for unit entrainment in states of locomotion, but it may also be worth-while testing the strength of respiration-driven entrainment in this situation. In fact, theta and respiration can easily be confounded in mice due to their strongly overlapping frequency ranges [53].

It is unclear how respiration-entrained signals are transmitted to distant cortical brain areas. Clearly, feedback from the nasal airstream plays a role, since RR diminishes after tracheotomy [63], bulbectomy [4, 5], chemogenetic inhibition of the OB [38], depletion of the olfactory epithelium [33, 39] or nasal occlusion [39]. It may well be that mechanic stimulation of olfactory epithelial cells by the airflow [1] are critical for RR generation [53]. However, Karalis and Sirota [33] recently demonstrated that lesioning the olfactory epithelium abolishes RR at the field potential level but does not eliminate neuronal entrainment by respiration. This finding argues for additional non-nasal sources of respiration-related activity modulation, possibly by collateral discharges from the rhythm-generating respiratory networks in the brainstem. An additional possibility are direct mechanical effects on neuronal activity. Cortical neurons do react to weak mechanical stimulation [42], and mechanosensitive Piezo2 ion channels have recently been shown to be present in cortical pyramidal cells, opening the possibility that minor pressure fluctuations in the brain parenchyma may translate into rhythmic entrainment of activity [3, 14]. Mechanical transduction processes could likewise mediate the heartbeat-dependent modulation of activity [13, 25, 60] for which there is no central rhythm generator. Our present results on modulation of neuronal activity by respiration do not allow to distinguish between the different possible mechanisms which are, notably, not mutually exclusive. In any case, we confirm that the power of the local field

potential is not consistently correlated with the strength of unit entrainment [33], suggesting that lamina-specific synaptic input is not the only mechanism of respiration-entrained neuronal discharges. Which of the two other mechanisms (corollary discharges from brainstem rhythm generators or mechanical stimulation of pyramidal cells) is responsible for the observed modulation of neuronal activity remains presently unclear.

Respiration-related network activity is a brain-wide phenomenon [57], and respiratory modulation of unit activity was demonstrated in a large number of brain regions [4, 5, 12, 32, 33, 35, 63]. This poses the question of its putative role for brain function. It has been suggested that the brain-wide coordination of activity by slow network oscillations contributes to signal integration between different neuronal networks [15, 28, 31, 51]. Respiration-related network oscillations (RR) may provide such a synchronizing signal, independent from their immediate relation to respiration or olfaction. The parietal cortex was found to play a critical role in decision-making processes [2, 22, 36, 40, 43] that strongly rely on the brain-wide integration of sensory information, behavioral and internal state and intended actions. It seems possible that RR provides a temporal scaffold for the underlying computations in the parietal cortex. Moreover, the parietal cortex serves important roles in spatial navigation [22, 36, 61]. Whether spatial cognition is specifically modulated by respiration is currently unknown, but would be well compatible with our present findings, especially the state-dependent expression of RR and its coordination with θ oscillations. A closely related cognitive process is spatial or declarative memory formation [9]. Of note, respiratory signals modulate hippocampal sharp-wave ripples [33, 38] – a biomarker of memory consolidation [8] – implicating a role of respiration in the underlying processes [16, 23]. Importantly, the presence of localized, concurrent ripple oscillations in the parietal cortex was recently observed in rats [34] possibly aiding information transfer from hippocampal to neocortical networks during memory consolidation. Interestingly, a recent study by Tingley and colleagues [52] found that hippocampal sharp wave-ripples additionally influence metabolic processes, highlighting the embeddedness of brain function within the whole body [50, 58] in which respiratory signals potentially serve a critical role [59].

Taken together, accumulating evidence shows the impact of bodily signals such as respiration on brain dynamics, opening possibilities to formulate and test novel hypotheses on the interaction between neuronal activity, behavior and cognition. In addition, our present findings underline the state-dependence of entrainment of neocortical neurons, which can be driven by θ, respiration or both oscillations depending on firing rate and behavioral state.

Declarations

Data availability

The data will be available upon request.

Acknowledgement

We thank Katja Lankisch for expert technical assistance.

Funding

This work was supported by the German Research Foundation (DR 326 15-1), the Brazilian National Council for Scientific and Technological Development (CNPq 308653/2018-1; 408508/2018-3), the Brazilian Coordination for the Improvement of Higher Education Personal (CAPES 99999.000558/2016-08), and the Alexander von Humboldt Foundation.

Competing interests

The authors have no financial or non-financial interests to declare.

Author contributions

FJ and YY performed experiments, contributed to data analysis, figures and manuscript writing. JB designed experiments and performed data analysis, validation of results and manuscript writing. ABLT designed and applied advanced methods of data analysis. AD supervised the laboratory work and finalized the manuscript. All authors reviewed the manuscript.

References

1. Adrian ED (1942) Olfactory reactions in the brain of the hedgehog. J Physiol 100:459–473. doi: 10.1113/jphysiol.1942.sp003955
2. Akrami A, Kopec CD, Diamond ME, Brody CD (2018) Posterior parietal cortex represents sensory history and mediates its effects on behaviour. Nature 554:368–372. doi: 10.1038/nature25510
3. An C, Qi H, Wang L, Fu X, Wang A, Wang ZL, Liu J (2021) Piezotronic and piezo-phototronic effects of atomically-thin ZnO nanosheets. Nano Energy 82:105653. doi: 10.1016/j.nanoen.2020.105653
4. Bagur S, Lefort JM, Lacroix MM, de Lavilléon G, Herry C, Chouvaeff M, Billand C, Geoffroy H, Benchenane K (2021) Breathing-driven prefrontal oscillations regulate maintenance of conditioned-fear evoked freezing independently of initiation. Nat Commun 12:1–15. doi: 10.1038/s41467-021-22798-6
5. Biskamp J, Bartos M, Sauer JF (2017) Organization of prefrontal network activity by respiration-related oscillations. Sci Rep 7:1–11. doi: 10.1038/srep45508
6. Bott JB, Muller MA, Jackson J, Aubert J, Cassel JC, Mathis C, Goutagny R (2016) Spatial reference memory is associated with modulation of theta-gamma coupling in the dentate Gyrus. Cereb Cortex 26:3744–3753. doi: 10.1093/cercor/bhv177
7. Brankačk J, Kukushka VI, Vyssotski AL, Draguhn A (2010) EEG gamma frequency and sleep-wake scoring in mice: Comparing two types of supervised classifiers. Brain Res 1322:59–71. doi: 10.1016/j.brainres.2010.01.069
8. Buzsáki G (2015) Hippocampal sharp wave-ripple: A cognitive biomarker for episodic memory and planning. Hippocampus 25:1073–1188. doi: 10.1002/hipo.22488

9. Buzsáki G, Moser EI (2013) Memory, navigation and theta rhythm in the hippocampal-entorhinal system. Nat Neurosci 16:130–138. doi: 10.1038/nn.3304
10. Canolty RT, Knight RT (2010) The functional role of cross-frequency coupling. Trends Cogn Sci 14:506–515. doi: 10.1016/j.tics.2010.09.001
11. Chaure FJ, Rey HG, Quian Quiroga R (2018) A novel and fully automatic spike-sorting implementation with variable number of features. J Neurophysiol 120:1859–1871. doi: 10.1152/jn.00339.2018
12. Chi VN, Müller C, Wolfenstetter T, Yanovsky Y, Draguhn A, Tort ABL, Brankačk J (2016) Hippocampal respiration-driven rhythm distinct from theta oscillations in awake mice. J Neurosci 36:162–177. doi: 10.1523/JNEUROSCI.2848-15.2016
13. Critchley HD, Garfinkel SN (2018) The influence of physiological signals on cognition. Curr Opin Behav Sci 19:13–18. doi: 10.1016/j.cobeha.2017.08.014
14. Draguhn A (2022) The Mechanics of the Brain. J Integr Neurosci. doi: 10.1038/scientificamerican10111873-224d
15. Draguhn A, Buzsáki G (2004) Neuronal Oscillations in Cortical Networks. Science (80-) 304:1926–1930
16. Folschweiller S, Sauer JF (2021) Respiration-Driven Brain Oscillations in Emotional Cognition. Front Neural Circuits 15:1–12. doi: 10.3389/fncir.2021.761812
17. Fries P (2009) Neuronal Gamma-Band Synchronization as a Fundamental Process in Cortical Computation. Annu Rev Neurosci 32:209–224. doi: 10.1146/annurev.neuro.051508.135603
18. Fries P (2015) Rhythms for Cognition: Communication through Coherence. Neuron 88:220–235. doi: 10.1016/j.neuron.2015.09.034
19. Girin B, Juventin M, Garcia S, Lefèvre L, Amat C, Fourcaud-Trocmé N, Buonviso N (2021) The deep and slow breathing characterizing rest favors brain respiratory-drive. Sci Rep 11:1–15. doi: 10.1038/s41598-021-86525-3
20. Hammer M, Schwale C, Brankačk J, Draguhn A, Tort ABL (2021) Theta-gamma coupling during REM sleep depends on breathing rate. Sleep 44:1–12. doi: doi:10.1093/sleep/zsab189
21. Harris KD, Quiroga RQ, Freeman J, Smith SL (2016) Improving data quality in neuronal population recordings. Nat Neurosci 19:1165–1174. doi: 10.1038/nn.4365
22. Harvey CD, Coen P, Tank DW (2012) Choice-specific sequences in parietal cortex during a virtual-navigation decision task. Nature 484:62–68. doi: 10.1038/nature10918
23. Heck DH, Kozma R, Kay LM (2019) The rhythm of memory: How breathing shapes memory function. J Neurophysiol 122:563–571. doi: 10.1152/jn.00200.2019
24. Helfrich RF, Knight RT (2016) Oscillatory dynamics of prefrontal cognitive control. Trends Cogn Sci 20:916–930. doi: http://dx.doi.org/10.1016/j.tics.2016.09.007
25. Herman AM, Tsakiris M (2021) The impact of cardiac afferent signaling and interoceptive abilities on passive information sampling. Int J Psychophysiol 162:104–111. doi: 10.1016/j.ijpsycho.2021.02.010

26. Herrero JL, Khuvis S, Yeagle E, Cerf M, Mehta AD (2018) Breathing above the brain stem: Volitional control and attentional modulation in humans. J Neurophysiol 119:145–159. doi: 10.1152/jn.00551.2017
27. Hill DN, Mehta SB, Kleinfeld D (2011) Quality metrics to accompany spike sorting of extracellular signals. J Neurosci 31:8699–8705. doi: 10.1523/JNEUROSCI.0971-11.2011
28. Hyafil A, Giraud AL, Fontolan L, Gutkin B (2015) Neural Cross-Frequency Coupling: Connecting Architectures, Mechanisms, and Functions. Trends Neurosci 38:725–740. doi: 10.1016/j.tins.2015.09.001
29. Ito J, Roy S, Liu Y, Cao Y, Fletcher M, Lu L, Boughter JD, Grün S, Heck DH (2014) Whisker barrel cortex delta oscillations and gamma power in the awake mouse are linked to respiration. Nat Commun 5:1–10. doi: 10.1038/ncomms4572
30. Jessberger J, Zhong W, Brankačk J, Draguhn A (2016) Olfactory Bulb Field Potentials and Respiration in Sleep-Wake States of Mice. Neural Plast 2016. doi: 10.1155/2016/4570831
31. Jung F, Carlén M (2021) Neuronal oscillations and the mouse prefrontal cortex. Int Rev Neurobiol 158:337–372. doi: 10.1016/bs.irn.2020.11.005
32. Jung F, Witte V, Yanovsky Y, Klumpp M, Brankačk J, Tort ABL, Draguhn A (2022) Differential modulation of parietal cortex activity by respiration and θ-oscillations. J Neurophysiol
33. Karalis N, Sirota A (2022) Breathing coordinates cortico-hippocampal dynamics in mice during offline states. Nat Commun 13:467. doi: 10.1038/s41467-022-28090-5
34. Khodagholy D, Gelinas JN, Buzsáki G (2017) Learning-enhanced coupling between ripple oscillations in association cortices and hippocampus. Science (80-) 358:369–372
35. Kőszeghy Á, Lasztóczi B, Forro T, Klausberger T (2018) Spike-timing of orbitofrontal neurons is synchronized with breathing. Front Cell Neurosci 12:1–12. doi: 10.3389/fncel.2018.00105
36. Krumin M, Lee JJ, Harris KD, Carandini M (2017) Decision and navigation in mouse parietal cortex. bioRxiv 1–18. doi: 10.1101/166413
37. Lisman JE, Jensen O (2013) The Theta-Gamma Neural Code. Neuron 77:1002–1016. doi: 10.1016/j.neuron.2013.03.007
38. Liu Y, McAfee SS, Heck DH (2017) Hippocampal sharp-wave ripples in awake mice are entrained by respiration. Sci Rep 7:1–9. doi: 10.1038/s41598-017-09511-8
39. Moberly AH, Schreck M, Bhattarai JP, Zweifel LS, Luo W, Ma M (2018) Olfactory inputs modulate respiration-related rhythmic activity in the prefrontal cortex and freezing behavior. Nat Commun 9. doi: 10.1038/s41467-018-03988-1
40. Najafi F, Elsayed GF, Cao R, Pnevmatikakis E, Latham PE, Cunningham JP, Churchland AK (2020) Excitatory and Inhibitory Subnetworks Are Equally Selective during Decision-Making and Emerge Simultaneously during Learning. Neuron 105:165-179.e8. doi: 10.1016/j.neuron.2019.09.045
41. Nakamura NH, Fukunaga M, Oku Y (2018) Respiratory modulation of cognitive performance during the retrieval process. PLoS One 13:1–17. doi: 10.1371/journal.pone.0204021

42. Nikolaev YA, Dosen PJ, Laver DR, Van Helden DF, Hamill OP (2015) Single mechanically-gated cation channel currents can trigger action potentials in neocortical and hippocampal pyramidal neurons. Brain Res 1608:1–13. doi: 10.1016/j.brainres.2015.02.051
43. Pho GN, Goard MJ, Woodson J, Crawford B, Sur M (2018) Task-dependent representations of stimulus and choice in mouse parietal cortex. Nat Commun 9. doi: 10.1038/s41467-018-05012-y
44. Quiroga R, Nadasdy Z, Ben-Shaul Y (2004) Unsupervised spike detection and sorting with wavelets and superparamagnetic clustering. Neural Comput 16:1661–1687. doi: 10.1162/089976604774201631
45. Rebollo I, Devauchelle AD, Béranger B, Tallon-Baudry C (2018) Stomach-brain synchrony reveals a novel, delayed-connectivity resting-state network in humans. Elife 7:1–25. doi: 10.7554/eLife.33321
46. Richter CG, Babo-Rebelo M, Schwartz D, Tallon-Baudry C (2017) Phase-amplitude coupling at the organism level: The amplitude of spontaneous alpha rhythm fluctuations varies with the phase of the infra-slow gastric basal rhythm. Neuroimage 146:951–958. doi: 10.1016/j.neuroimage.2016.08.043
47. Rojas-Líbano D, Del Solar JW, Aguilar-Rivera M, Montefusco-Siegmund R, Maldonado PE (2018) Local cortical activity of distant brain areas can phase-lock to the olfactory bulb's respiratory rhythm in the freely behaving rat. J Neurophysiol 120:960–972. doi: 10.1152/jn.00088.2018
48. Scheffzük C, Kukushka VI, Vyssotski AL, Draguhn A, Tort ABL, Brankačk J (2011) Selective coupling between theta phase and neocortical fast gamma oscillations during REM-sleep in mice. PLoS One 6:1–9. doi: 10.1371/journal.pone.0028489
49. Schmitzer-Torbert N, Jackson J, Henze D, Harris K, Redish AD (2005) Quantitative measures of cluster quality for use in extracellular recordings. Neuroscience 131:1–11. doi: 10.1016/j.neuroscience.2004.09.066
50. Shapiro L (2011) Embodied Cognition. New Problems in Philosophy. Routledge, New York, NY, USA
51. Sirota A, Montgomery S, Fujisawa S, Isomura Y, Zugaro M, Buzsáki G (2008) Entrainment of Neocortical Neurons and Gamma Oscillations by the Hippocampal Theta Rhythm. Neuron 60:683–697. doi: 10.1016/j.neuron.2008.09.014
52. Tingley D, McClain K, Kaya E, Carpenter J, Buzsáki G (2021) A metabolic function of the hippocampal sharp wave-ripple. Nature 597:82–86. doi: 10.1038/s41586-021-03811-w
53. Tort ABL, Brankačk J, Draguhn A (2018) Respiration-Entrained Brain Rhythms Are Global but Often Overlooked. Trends Neurosci 41:186–197. doi: 10.1016/j.tins.2018.01.007
54. Tort ABL, Hammer M, Zhang J, Brankačk J, Draguhn A (2021) Temporal relations between cortical network oscillations and breathing frequency during REM sleep. J Neurosci 41:5229–5242. doi: 10.1523/JNEUROSCI.3067-20.2021
55. Tort ABL, Komorowski RW, Manns JR, Kopell NJ, Eichenbaum H (2009) Theta-gamma coupling increases during the learning of item-context associations. Proc Natl Acad Sci 106:20942–20947. doi: 10.1073/pnas.0911331106

56. Tort ABL, Kramer MA, Thorn C, Gibson DJ, Kubota Y, Graybiel AM, Kopell NJ (2008) Dynamic cross-frequency couplings of local field potential oscillations in rat striatum and hippocampus during performance of a T-maze task. Proc Natl Acad Sci 105:20517–20522. doi: 10.1073/pnas.0810524105
57. Tort ABL, Ponsel S, Jessberger J, Yanovsky Y, Brankačk J, Draguhn A (2018) Parallel detection of theta and respiration-coupled oscillations throughout the mouse brain. Sci Rep 8:1–14. doi: 10.1038/s41598-018-24629-z
58. Varela FJ, Rosch E, Thompson E (1991) The Embodied Mind. Cognitive Science and Human Experience. MIT Press, Cambridge, MA, USA
59. Varga S, Heck DH (2017) Rhythms of the body, rhythms of the brain: Respiration, neural oscillations, and embodied cognition. Conscious Cogn 56:77–90. doi: 10.1016/j.concog.2017.09.008
60. Waselius T, Wikgren J, Halkola H, Penttonen M, Nokia MS (2018) Learning by heart: Cardiac cycle reveals an effective time window for learning. J Neurophysiol 120:830–838. doi: 10.1152/jn.00128.2018
61. Whitlock JR, Sutherland RJ, Witter MP, Moser MB, Moser EI (2008) Navigating from hippocampus to parietal cortex. Proc Natl Acad Sci U S A 105:14755–14762. doi: 10.1073/pnas.0804216105
62. Yackle K, Schwarz LA, Kam K, Sorokin JM, Huguenard JR, Feldman JL, Luo L, Krasnow MA (2017) Breathing control center neurons that promote arousal in mice. Science (80-) 355:1411–1415. doi: doi:10.1126/science.aai7984
63. Yanovsky Y, Ciatipis M, Draguhn A, Tort ABL, Brankačk J (2014) Slow oscillations in the mouse hippocampus entrained by nasal respiration. J Neurosci 34:5949–5964. doi: 10.1523/JNEUROSCI.5287-13.2014
64. Zelano C, Jiang H, Zhou G, Arora N, Schuele S, Rosenow J, Gottfried JA (2016) Nasal respiration entrains human limbic oscillations and modulates cognitive function. J Neurosci 36:12448–12467. doi: 10.1523/JNEUROSCI.2586-16.2016
65. Zhong W, Ciatipis M, Wolfenstetter T, Jessberger J, Müller C, Ponsel S, Yanovsky Y, Brankačk J, Tort ABL, Draguhn A (2017) Selective entrainment of gamma subbands by different slow network oscillations. Proc Natl Acad Sci U S A 114:4519–4524. doi: 10.1073/pnas.1617249114

Figures

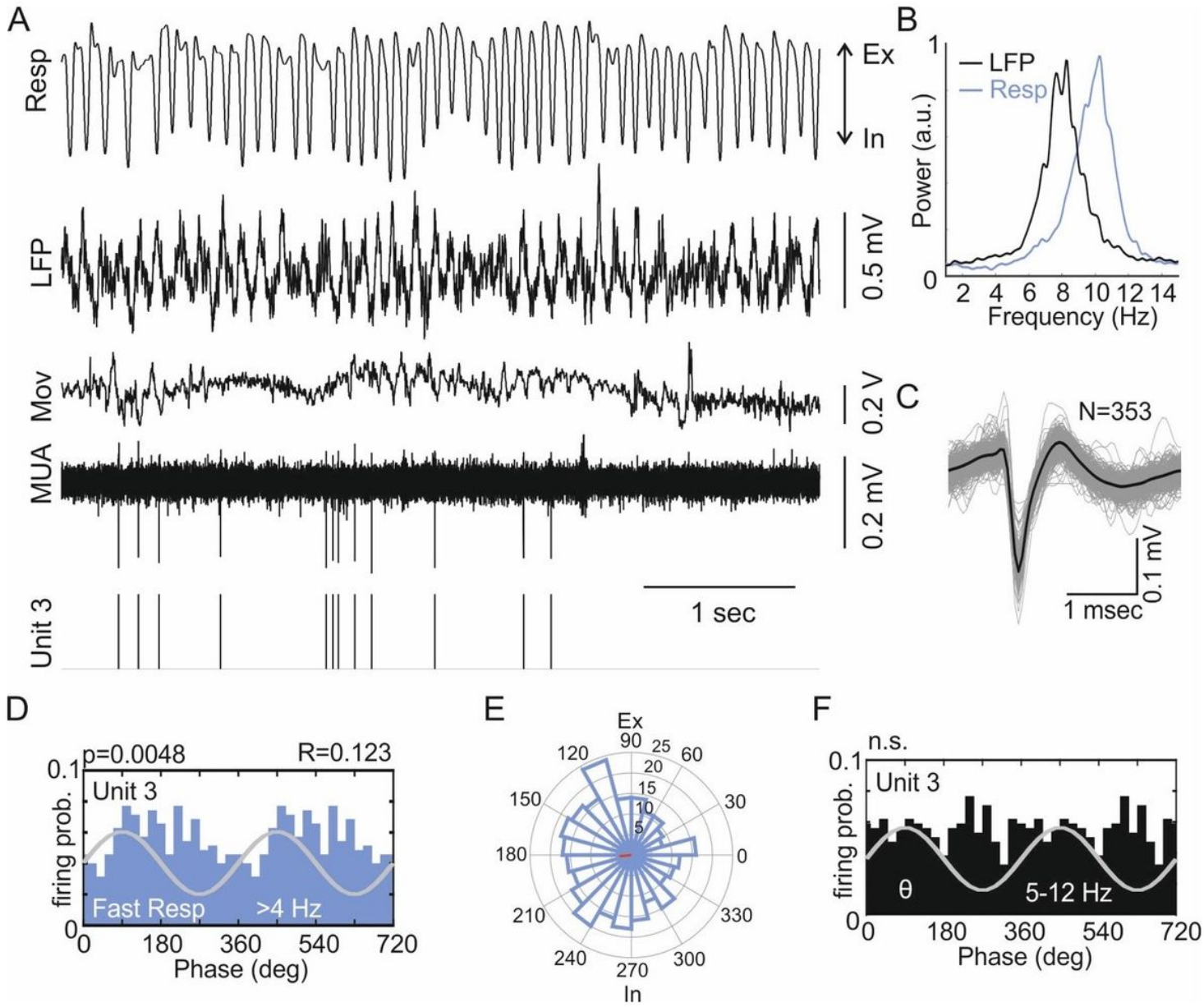

Figure 1

Parietal cortex unit modulated by fast respiration during active waking. A: Raw respiration (Resp) signal, local field potential (LFP) from the parietal cortex, accelerometer activity indicating movement (Mov), multi-unit-activity (MUA) from one tetrode wire, and the time stamps of a sorted and quality tested unit (unit 3) during active waking. **B**: Power spectra of the parietal cortex LFP (black) and Resp (blue) during active waking. θ and Resp are partly overlapping, yet with different frequencies of maximal power (Resp > θ). **C**: Averaged unit waveform (black) on the background of superimposed 353 single spikes (gray). **D**: Phase histogram of unit 3 firing probability based on Resp cycles (frequency range 4 - 14 Hz; 'fast respiration'). Note significant modulation of unit discharges by fast respiration. R indicates coupling strength. **E**: Polar plot showing Resp phase-dependent activation of unit 3. The firing probability is maximal between 90 (maximum of expiration, Ex) and 270 degrees (maximum of inspiration, In). **F**: Phase histogram of unit 3 based on θ cycles; the unit was not significantly modulated by θ (5 – 12 Hz).

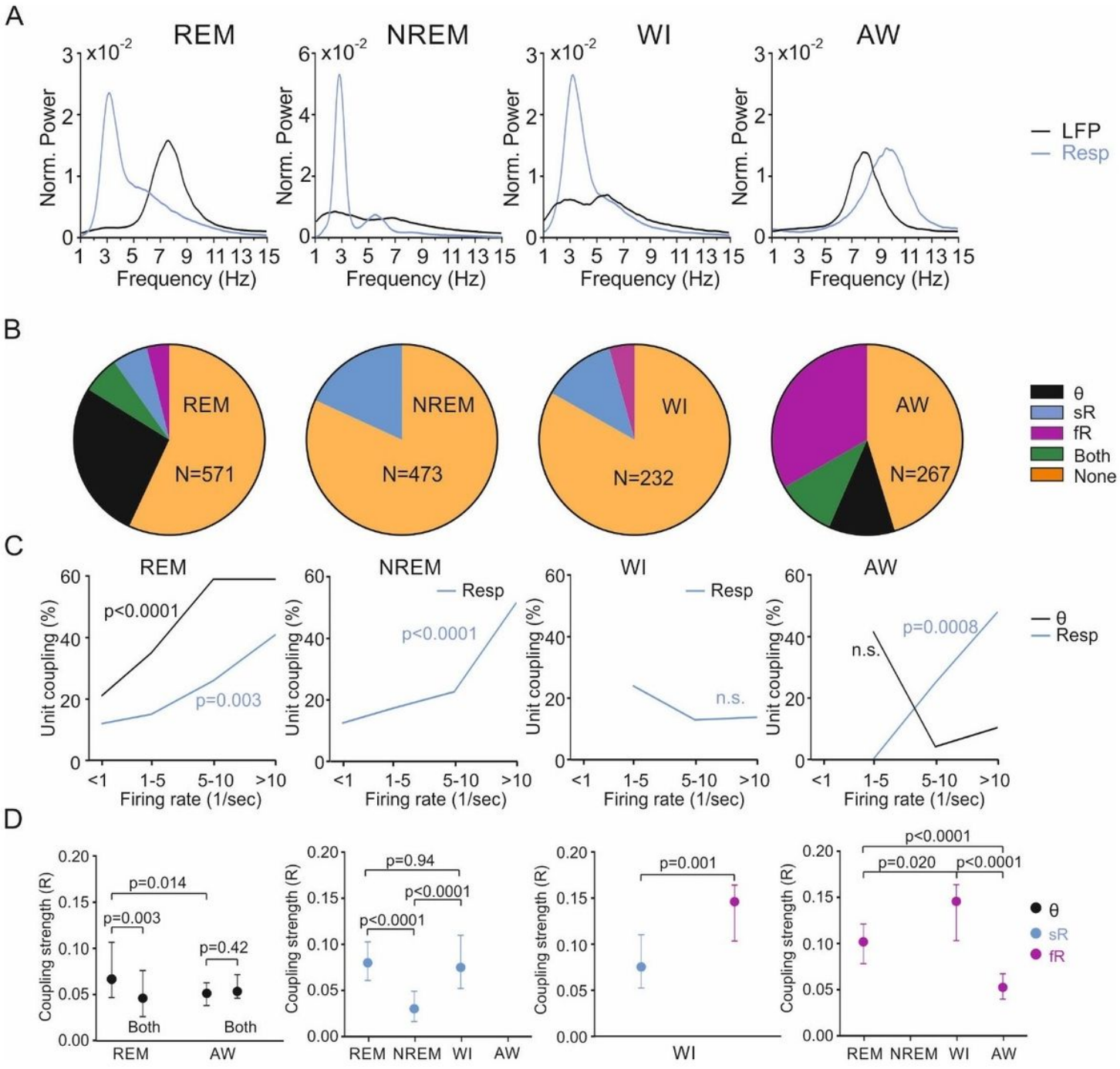

Figure 2

Modulation of parietal cortex units by θ and respiration in sleep and wakefulness. A: Mean power of slow rhythms (Resp, blue; θ, black) during REM sleep, NREM sleep, waking immobility (WI) and active waking (AW). Note absence of θ activity in NREM sleep and WI. **B**: Percentage of units modulated by θ (black), slow Resp (sR, blue), fast Resp (fR, magenta) or θ and Resp (sR and fR) simultaneously ("Both", green). Orange indicates non-modulated units. Note that θ-modulation dominates in REM sleep whereas modulation by fR prevails in AW. **C**: Relation between firing rate and unit coupling to θ or Resp. Coupling to θ increases significantly with firing rate in REM but not in AW. Unit modulation by Resp increases significantly with firing rate in REM, NREM and AW but does not change in WI (see Table 1 for details). **D**:

Coupling strength of units to θ (black dots and errors: 25% and 75% percentiles) and respiration (blue dots and errors: sR, magenta dots: fR). Differences in coupling strength for the respective states are indicated by brackets and p-values.

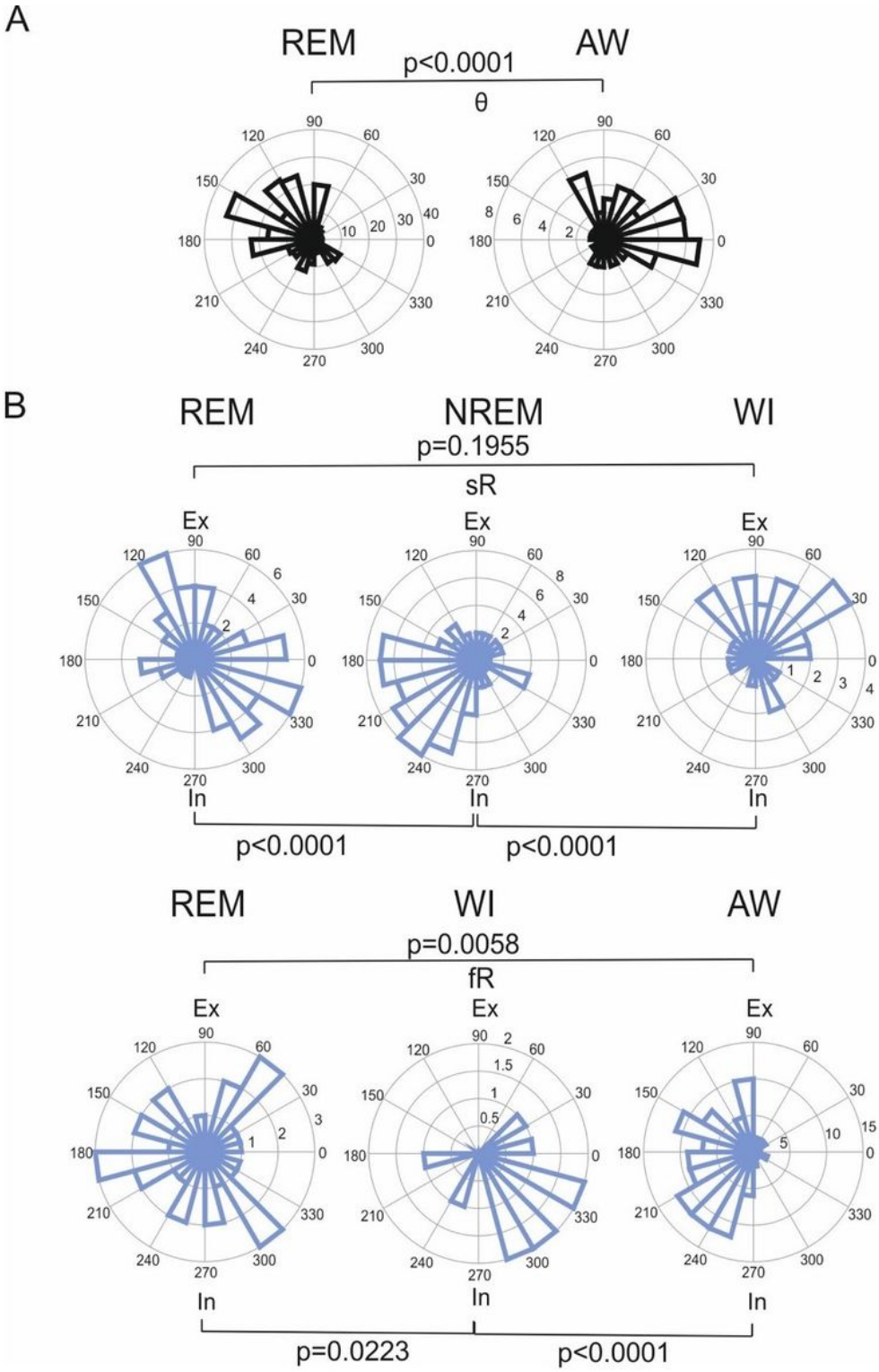

Figure 3

State-dependent phase preference of parietal cortex. A: Units modulated by θ have significantly different θ phase preferences in REM compared to AW. **B**: Units coupled to slow respiration (sR) are entrained to different phases of respiration in REM compared to WI; units in NREM preferentially fire during the rising flank of inspiration (In, 180 to 270 deg), whereas units in WI fire mostly during expiration (Ex, 0 to 180 deg). In AW, units modulated by fast Resp (fR) preferentially fire during the rising flank of In and the falling flank of Ex. P values are based on the Watson U2 test.